# Isobaric Vapor−Liquid Equilibria for the Systems Propionic Acid + Butyric Acid, Isobutyric Acid + Butyric Acid, Butyric Acid + Isovaleric Acid, and Butyric Acid + Hexanoic Acid at 14 kPa

**Reshan Sewnarain, Deresh Ramjugernath,* and J. David Raal**

Thermodynamics Research Unit, School of Chemical Engineering, University of Natal, Durban 4001, South Africa

Isobaric vapor−liquid equilibria were measured at 14 kPa for the binary systems propionic acid + butyric acid, isobutyric acid + butyric acid, butyric acid + isovaleric acid, and butyric acid + hexanoic acid. The experimental data were modeled using the $\gamma-\varphi$ approach as discussed by Raal and Mühlbauer. The proposed model uses the NRTL equation for correlation of the liquid-phase activity coefficient. The vapor-phase fugacity coefficient was calculated by the chemical theory, which treats binary mixtures containing associating species. The data were deemed thermodynamically consistent using a test proposed by Van Ness.

## 1. Introduction

Large streams of mixed carboxylic acids (consisting mostly of butyric acid) are produced by local industry, and a study was undertaken of the feasibility of their separation by distillation. Therefore, vapor−liquid equilibrium data were required for key pairs of these acids. A literature survey revealed that data were scarce for systems involving butyric acid with other acids. The only system available in the literature was for the binary system butyric acid + valeric acid as cited by Gmehling et al.[3] Therefore, isobaric vapor−liquid equilibrium data were measured for the systems propionic acid + butyric acid, isobutyric acid + butyric acid, butyric acid + isovaleric acid, and butyric acid + hexanoic acid at 14 kPa.

## 2. Experimental Section

***Materials.*** Butyric acid was purchased from Riedel−de Haën, and the remaining acids were purchased from Fluca Enterprises. The reagents were used without further purification after gas chromatographic analysis showed no significant impurities. The purities of the reagents were also checked by their refractive indices, and comparisons with literature values are shown in Table 1.

***Apparatus and Procedure.*** A block diagram of the experimental setup is shown in Figure 1. The various components of the experimental setup include a VLE still, Schott 10 L and Pyrex 5 L ballast flasks, a TECHNE cold finger, a Fischer VKH 100 pressure controller, a LABOTEC water bath with a glycol + water mixture, and two pumps.

A highly refined dynamic VLE still (Figure 2) has been developed by Raal and Mühlbauer[1] and is described in detail by Joseph.[4] The still is suitable for low-pressure measurements. Features worth noting are as follows:

(a) Packing is used in the equilibrium chamber to ensure rapid attainment of equilibrium due to intimate contact between the vapor and the liquid and the expansion of the interfacial surface area. Constant vapor and liquid compositions and a constant temperature verify equilibrium conditions.

* Corresponding author. E-mail: ramjuger@nu.ac.za.

**Table 1. Refractive Indexes and Purities of Components**

| reagent | refractive index (293.15 K) exp | refractive index (293.15 K) lit.[a] | min purity (mass %)[b] |
|---|---|---|---|
| butyric acid | 1.3978 | 1.3980 | 99 |
| isobutyric acid | 1.3935 | 1.3930 | 99 |
| propionic acid | 1.3807 | 1.3809 | 99 |
| isovaleric acid | 1.4025 | 1.4030 | 98 |
| hexanoic acid | 1.4169 | 1.4163 | 99 |

[a] Reference 9. [b] As stated by supplier.

(b) Stirring in the condensate receiver eliminates temperature and concentration gradients. This ensures high reproducibility of the vapor sample concentrations.

(c) Stirring in the boiling chamber (not shown in Figure 2) ensures thorough mixing of the returning condensate before evaporation. This prevents "flashing" and produces smooth boiling.

(d) A system of internal and external heaters is used in the boiling chambers to ensure rapid boiling, permit precise control of the circulation rate, and provide nucleation sites for smooth boiling.

A Eurotherm temperature indicator was used to display the resistance of the Pt-100 temperature sensor. The pressure was monitored with a Fischer pressure transducer. The uncertainties of the temperature and pressure measurements are estimated to be ±0.02 K and ±0.03 kPa, respectively.

For isobaric operation the pressure is maintained at a constant set-point that is controlled by a Fischer pressure controller which either vents to the atmosphere through needle valve $V_2$ or connects to the vacuum pump through solenoid valve $V_1$. By actuation of the solenoid valve, leading to a vacuum pump and the atmosphere, the pressure in the still can be controlled. Control of the still pressure is estimated to be within ±0.1% of the set-point pressure.

The equilibrium compositions of the samples were determined using a Varian, Model 3300, gas chromatograph (GC). The column used was a 30-m megabore capillary column of 0.53-mm diameter with Poropak Q on fused silica. A flame ionization detector was used. Analyses were

10.1021/je0102412 CCC: $22.00 
Published on Web 04/03/2002

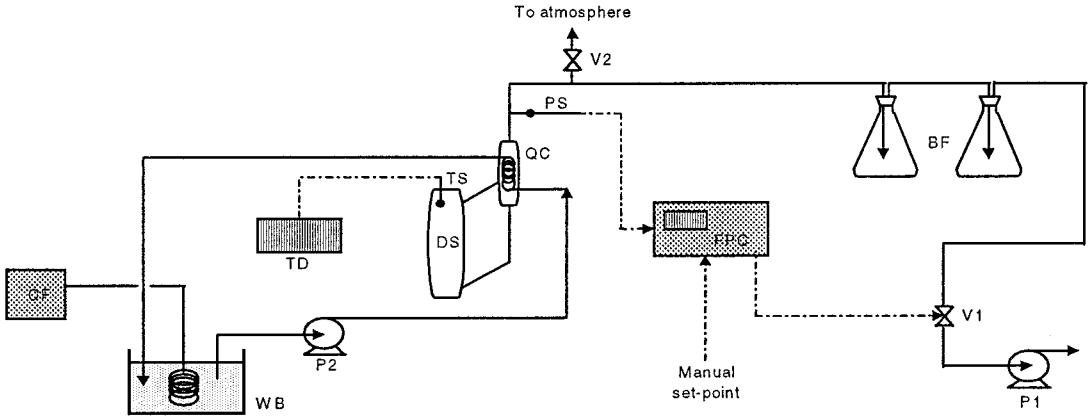


**Figure 1.** Schematic diagram of the VLE apparatus setup: BF, Schott 10 L and Pyrex 5 L ballast flasks; CF, TECHNE cold finger; DS, dynamic VLE still (Raal modification); FPT, Fischer Vakuum-Konstanthalter VKH 100 pressure controller; P1, pump 1; P2, pump 2; PS, Fischer pressure sensor; QC, Pyrex glass condenser; TD, Eurotherm temperature display; TS, Pt-100 temperature sensor; V1, solenoid valve; V2, needle valve; WB, LABOTEC water bath with glycol−water mix.

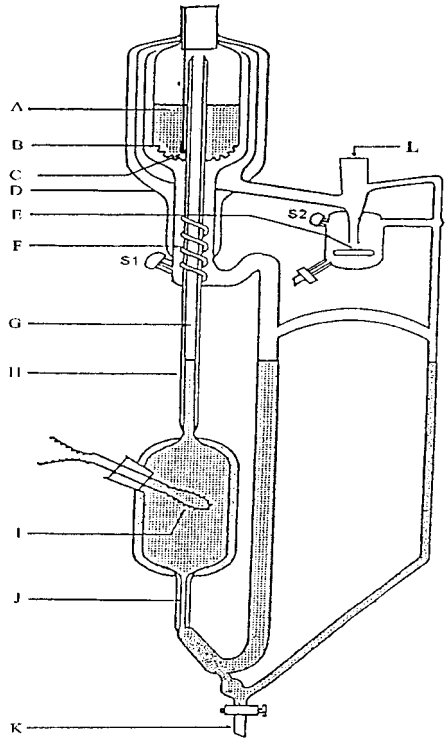


**Figure 2.** Schematic diagram of the vapor−liquid equilibrium still: A, SS wire mesh packing; B, drain holes; C, Pt-100 bulb; D, vacuum jacket; E, magnetic stirrer; F, SS mixing spiral; G, insulated Cottrell pump; H, vacuum jacket; I, internal heater; J, capillary; K, drain valve; S1, liquid sampling point; S2, vapor sampling point; L, condenser attachment joint.

based on the GC area ratio method, which is discussed in ref 1. The estimated accuracy of composition measurements is ±0.001 mole fraction.

## 3. Results and Discussion

Isobaric VLE data were measured for binary systems of butyric acid with isobutyric acid, propionic acid, isovaleric acid, and hexanoic acid at 14 kPa. These data sets are listed in Table 3 and plotted in Figures 3−10.

The isobaric VLE data were modeled using the $\gamma-\varphi$ approach as described by Raal and Mühlbauer.[1] Various models for liquid-phase association have been proposed (e.g. that in ref 5), but it was not the purpose of the present study to test liquid-phase association models. Association

**Table 2. Antoine Coefficients for Equation 7**

| chemical name | $A_i$ | $B_i$ | $C_i$ |
|---|---|---|---|
| propionic acid | 7.5 | 2000 | −151.1 |
| butyric acid | 7.7 | 1999.98 | −177.3 |
| isovaleric acid | 7.6 | 2000 | −186.3 |
| isobutyric acid | 7.6 | 1999.3 | −163.8 |
| hexanoic acid | 3.6328 | 487.9496 | −328.995 |

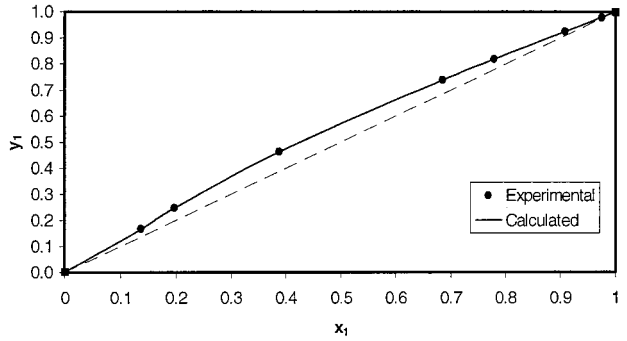


**Figure 3.** $x-y$ curve for isobutyric acid (1) + butyric acid (2).

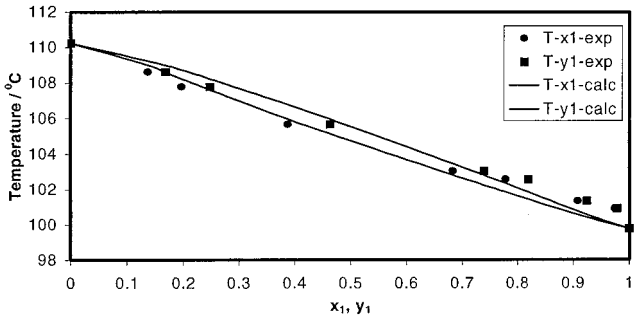


**Figure 4.** $T-x-y$ curve for isobutyric acid (1) + butyric acid (2).

in the vapor phase must, however, be accounted for in the calculation of activity coefficients.

For VLE, a vapor phase (V) and liquid phase (L) are in equilibrium at the same temperature and pressure when their respective fugacities ($f_i$) are equal:

$$\hat{f}_i^{\,V} = \hat{f}_i^{\,L} \tag{1}$$

Because of the strong nonidealities in carboxylic acid vapors, vapor-phase fugacity coefficients were calculated using the virial equations for vapor-phase chemical associations as described by Prausnitz et al.[5] Carboxylic acids

**Table 3. Experimental Vapor−Liquid Equilibrium Temperature *T*, Vapor Mole Fraction $\gamma_i$, and Activity Coefficients $\gamma_i$ at 14 kPa as a Function of Liquid Mole Fraction $x_i$**

| $x_1$ | $y_1$ | $T$/K | $\gamma_1$ | $\gamma_2$ |
|---|---|---|---|---|
| | | Propionic Acid (1) + Butyric Acid (2) | | |
| 1 | 1 | 361.32 | | 1.420[a] |
| 0.918 | 0.948 | 362.76 | 1.021 | 1.384 |
| 0.787 | 0.880 | 364.60 | 1.048 | 1.138 |
| 0.625 | 0.769 | 367.40 | 1.065 | 1.119 |
| 0.546 | 0.705 | 368.73 | 1.074 | 1.126 |
| 0.456 | 0.624 | 370.70 | 1.074 | 1.117 |
| 0.349 | 0.511 | 373.15 | 1.074 | 1.108 |
| 0.223 | 0.358 | 376.10 | 1.080 | 1.098 |
| 0.145 | 0.255 | 378.10 | 1.119 | 1.078 |
| 0 | 0 | 383.40 | 1.120[a] | |
| | | Isobutyric Acid (1) + Butyric Acid (2) | | |
| 1 | 1 | 372.16 | | 0.840[a] |
| 0.975 | 0.987 | 373.10 | 0.998 | 0.849 |
| 0.877 | 0.927 | 374.33 | 0.988 | 0.917 |
| 0.792 | 0.865 | 375.43 | 0.947 | 0.932 |
| 0.663 | 0.731 | 377.09 | 0.954 | 0.955 |
| 0.521 | 0.584 | 378.90 | 0.949 | 0.962 |
| 0.361 | 0.407 | 380.80 | 0.945 | 0.962 |
| 0.260 | 0.299 | 381.89 | 0.922 | 0.985 |
| 0.212 | 0.251 | 382.38 | 0.907 | 1.002 |
| 0 | 0 | 383.40 | 0890[a] | |
| | | Butyric Acid (1) + Isovaleric Acid (2) | | |
| 0 | 0 | 396.18 | 1.045[a] | |
| 0.034 | 0.052 | 394.83 | 1.041 | 1.000 |
| 0.082 | 0.119 | 394.12 | 1.033 | 1.001 |
| 0.196 | 0.266 | 392.56 | 1.017 | 1.003 |
| 0.521 | 0.615 | 388.83 | 1.000 | 1.011 |
| 0.683 | 0.759 | 387.18 | 0.999 | 1.012 |
| 0.810 | 0.858 | 385.95 | 0.999 | 1.020 |
| 0.895 | 0.918 | 385.15 | 0.999 | 1.021 |
| 1 | 1 | 383.40 | | 1.024[a] |
| | | Butyric Acid (1) + Hexanoic Acid (2) | | |
| 0 | 0 | 411.41 | 2.200[a] | |
| 0.042 | 0.192 | 410.47 | 2.125 | 1.292 |
| 0.154 | 0.511 | 401.95 | 1.672 | 1.336 |
| 0.323 | 0.732 | 395.86 | 1.383 | 1.536 |
| 0.545 | 0.835 | 391.62 | 1.199 | 2.122 |
| 0.625 | 0.853 | 390.39 | 1.166 | 2.326 |
| 0.856 | 0.970 | 386.82 | 1.092 | 2.677 |
| 1 | 1 | 383.40 | | 2.850[a] |

[a] Extrapolated values.

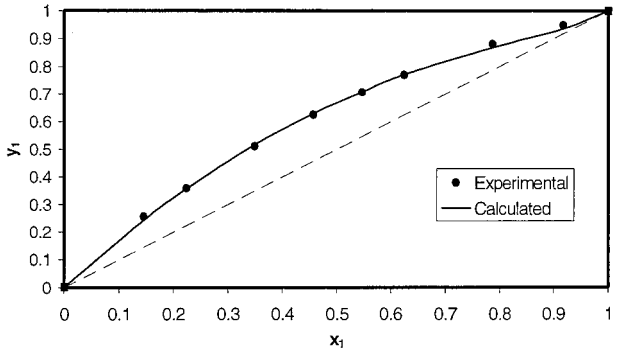


**Figure 5.** $x-y$ curve for propionic acid (1) + butyric acid (2).

tend to dimerize through strong hydrogen bonding. The hydrogen bonding process can be observed as a chemical reaction:

$$i + j \leftrightarrow ij \tag{2}$$

where $i$ and $j$ are monomer molecules and $ij$ is the complex (dimer) formed by hydrogen bonding. To describe the

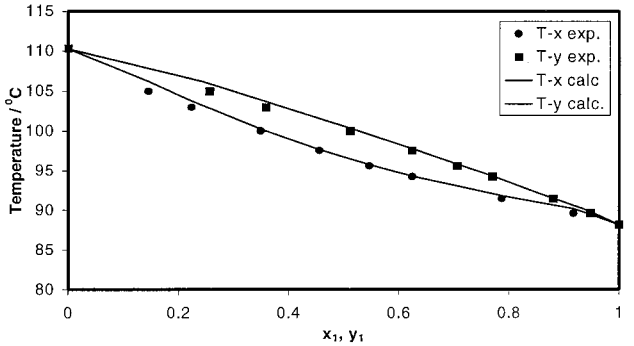


**Figure 6.** $T-x-y$ curve for propionic acid (1) + butyric acid (2).

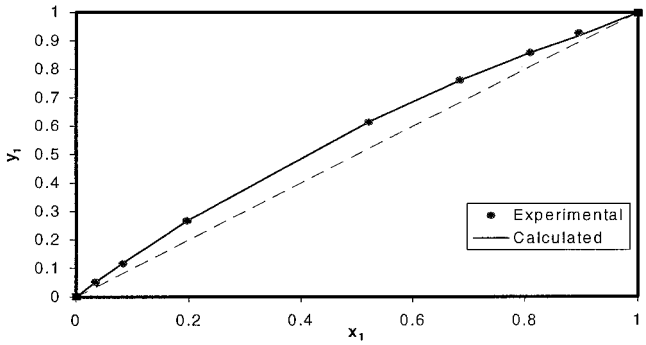


**Figure 7.** $x-y$ curve for butyric acid (1) + isovaleric acid (2).

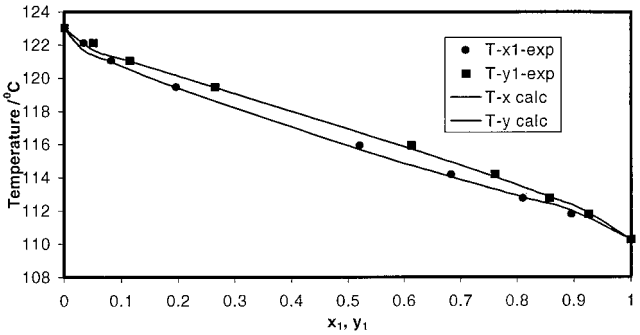


**Figure 8.** $T-x-y$ curve for butyric acid (1) + isovaleric acid (2).

chemical reaction, the following may be written:

$$k_{ij} = \frac{f_{ij}}{f_i f_j} = \frac{z_{ij}\phi^{\#}_{ij}}{P z_i z_j \phi^{\#}_i \phi^{\#}_j} \tag{3}$$

where $z$ is the true mole fraction of the species in equilibrium, $\phi^{\#}$ is the fugacity coefficient of the true species, $P$ is the system pressure, and $k_{ij}$ is the reaction equilibrium constant.

It has been shown by Nothnagel et al.[6] that the fugacity coefficient of component $i$ ($\phi_i$) is given by

$$\phi_i = \frac{z_i \phi^{\#}_i}{y_i} \tag{4}$$

where $y_i$ is defined as the apparent mole fraction of component $i$ in the vapor phase, neglecting dimerization.

If it is assumed that the vapor solution behaves like an ideal solution, the following may be written:

$$\ln \phi^{\#}_i = \frac{P B^{\mathrm{F}}_i}{RT} \tag{5}$$

**Table 4. Activity Coefficient Model Parameters ($g_{ij} - g_{ii}$) for the NRTL Equation and Calculated RMS $\delta$ ln($\gamma_1/\gamma_2$) Values for the Consistency Test**

| system | $g_{12} - g_{11}$ (cal·mol$^{-1}$) | $g_{12} - g_{22}$ (cal·mol$^{-1}$) | RMS $\delta$ ln($\gamma_1/\gamma_2$) |
|---|---|---|---|
| propionic acid (1) + butyric acid (2) | 1739.7 | −1077.6 | 0.098 |
| isobutyric acid (1) + butyric acid (2) | −795.8 | 1032.5 | 0.0625 |
| butyric acid (1) + isovaleric acid (2) | −652.282 | 807.304 | 0.0281 |
| butyric acid (1) + hexanoic acid (2) | 422.7335 | 224.106 | 0.3735 |

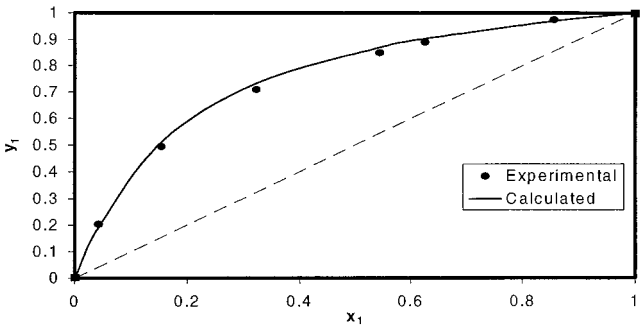


**Figure 9.** $x-y$ curve for butyric acid (1) + hexanoic acid (2).

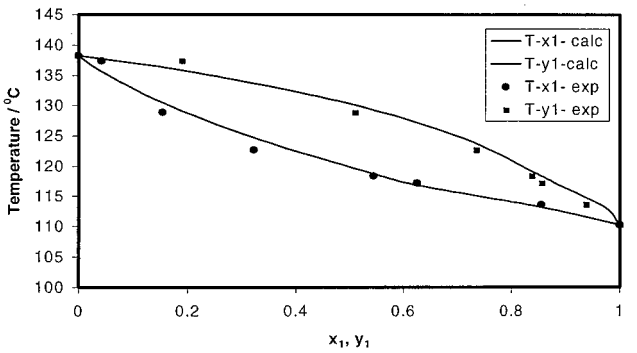


**Figure 10.** $T-x-y$ curve for butyric acid (1) + hexanoic acid (2).

where $B_i^F$ is the "free" contribution to the second virial equation as calculated by the Hayden and O'Connell method.[7]

The chemical equilibrium constant can be found from the relation

$$k_{ij} = \frac{-(2 - \delta_{ij})B_{ij}^D}{RT} \quad (6)$$

where $B_{ij}^D$ is the contribution of dimerization to the second virial coefficient as calculated by the Hayden and O'Connell method.[7] In the above equation $\delta_{ij} = 0$ ($i \neq j$), and $\delta_{ij} = 1$ ($i = j$). The calculation of the fugacity coefficient for components $i$ and $j$ is therefore accomplished by solving the above equations with the restriction that the sum of $z_i$, $z_j$, and $z_{ij}$ equals 1.

Vapor pressures ($P_i$) were calculated from the Antoine equation:

$$\log(P_i/\text{bar}) = A_i - \frac{B_i}{(T/\text{K}) + C_i} \quad (7)$$

and the constants $A_i$, $B_i$, and $C_i$ of each chemical are reported in Table 2.

The activity coefficients calculated from the experimental data, with fugacity coefficients calculated as described above, were correlated by means of the nonrandom two-liquid equation (NRTL equation).[5] This equation was convenient because it is converted readily to multicomponent systems and requires the least data for distillation simulations. The nonrandomness parameter $\alpha_{12}$ was set

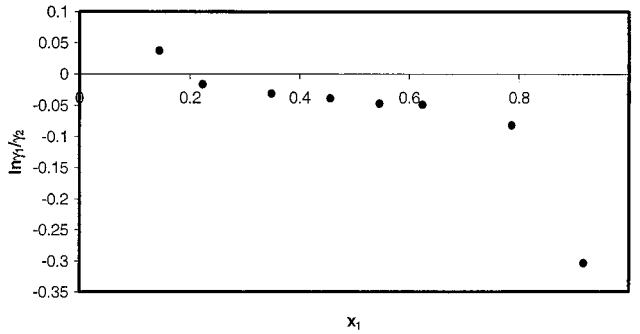


**Figure 11.** Plot of ln $\gamma_1/\gamma_2$ for propionic acid (1) + butyric acid (2).

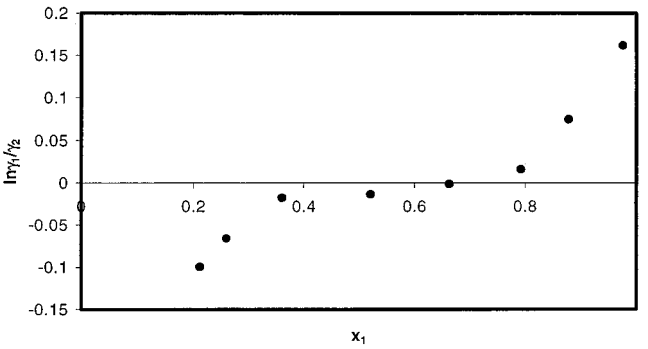


**Figure 12.** Plot of ln $\gamma_1/\gamma_2$ for isobutyric acid (1) + butyric acid (2).

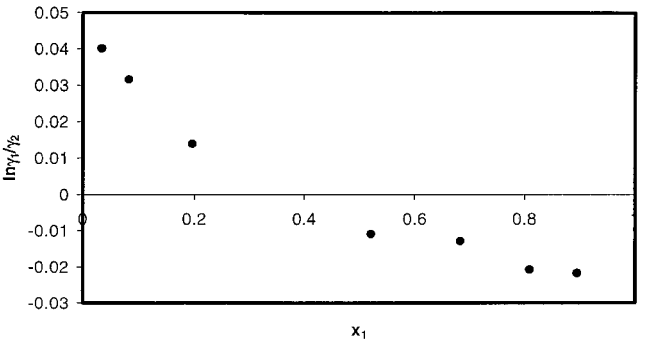


**Figure 13.** Plot of ln $\gamma_1/\gamma_2$ for butyric acid (1) + isovaleric acid (2).

equal to 0.2 after small variations around this value showed a mean deviation of only 0.001 mole fraction between calculated and correlated results. The NRTL interaction parameters were determined by the Marquardt method[8] and are shown in Table 4. The sum of squares of the difference between the calculated and measured excess Gibbs energies was minimized during the optimization of these parameters. The excess Gibbs energy was optimized to satisfy the requirements of the direct test of thermodynamic consistency proposed by Van Ness.[2] This procedure was used to test the experimental data for thermodynamic consistency. After minimization of the Gibbs energy function, calculation of the root-mean-square (RMS) value of $\delta$ ln($\gamma_1/\gamma_2$) is a measure of the consistency of the data (see

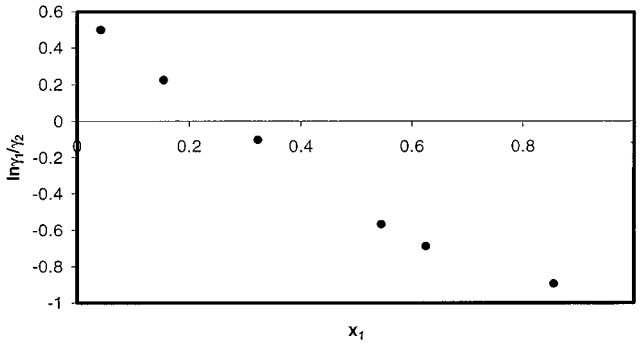


**Figure 14.** Plot of ln $\gamma_1/\gamma_2$ for butyric acid (1) + hexanoic acid (2).

Figures 11−14). According to Van Ness,[2] values greater than 0.2 imply inconsistent data. The calculated root-mean-square values are listed in Table 4 and show that all the systems measured were thermodynamically consistent except for the system butyric acid + hexanoic acid. The inconsistency for this system could possibly be attributed to the formation of trimers in the vapor phase, which would affect the calculated $\gamma_i$. The measured $T-x-y$ data should however still be useful for separation process design.

## 4. Conclusions

In this work, vapor−liquid equilibrium data have been measured for binary mixtures of carboxylic acids at 14 kPa. The isobaric data for the systems propionic acid + butyric acid, isobutyric acid + butyric acid, and butyric acid + isovaleric acid were found to be thermodynamically consistent. The data for the system butyric acid + hexanoic acid were not consistent.

## Literature Cited

(1) Raal, J. D.; Mühlbauer, A. L. *Phase Equilibria: Measurement and Computation*; Taylor and Francis: Bristol, PA, 1998.
(2) Van Ness, H. C. Thermodynamics in the treatment of Vapour/Liquid Equilibrium (VLE) Data. *Pure Appl. Chem.* **1995**, *67*, 859−872.
(3) Gmehling, J.; Onken, U. *Vapour Liquid Equilibrium Data Collection*, Vol. 1, Part 5; Dechema: Frankfurt/Main, 1982.
(4) Joseph, M. Computer-Aided Measurement of Vapour-Liquid Equilibria in a Dynamic Still at Sub-Atmospheric Pressures. MSc. Thesis, University of Natal, South Africa, 2001.
(5) Prausnitz, J. T.; Anderson, E.; Grens, C.; Eckert, R.; Hiesh; O'Connell, J. P. *Computer Calculations for Multicomponent Vapour-Liquid and Liquid−Liquid Equilibria*; Prentice Hall: Englewood Cliffs, NJ, 1980.
(6) Nothnagel, K. H.; Abrams, D. S.; Prausnitz, J. M. *Ind. Eng. Chem. Process Des. Dev.* **1973**, *12*, 25−35.
(7) Hayden, J. G.; O'Connell, J. P. *Ind. Eng. Chem. Process Des. Dev.* **1975**, *14*, 209−216.
(8) Marquardt, D. W. An Algorithm for least-squares estimation of nonlinear parameters. *J. Soc. Ind. Appl. Math.* **1963**, *11*, 431−441.
(9) Weast, R.; Grasselli, J. G. *Handbook of Chemistry and Physics*, 64th ed.; CRC Press: Boca Raton, FL, 1983−1984.

Received for review August 30, 2001. Accepted February 27, 2002. The authors wish to acknowledge the University of Natal Research Fund and Sasol (Pty) Ltd for funding this project.

JE0102412